JOURNAL OF CATALYSIS **168,** 1–15 (1997)
ARTICLE NO. CA971550

The Mechanism of Zeolite Y Destruction by Steam in the Presence of Vanadium

Carlos A. Trujillo,*[,1] Uriel Navarro Uribe,† Peter-Paul Knops-Gerrits,‡ Luis Alfredo Oviedo A.,* and Pierre A. Jacobs‡

*Laboratorio de Catálisis Heterogénea, Departamento de Química, Universidad Nacional de Colombia, Santafé de Bogotá, Colombia; †Instituto Colombiano del Petróleo, ICP, Bucaramanga, Santander, Colombia; and ‡Centrum voor Oppervlaktechemie en Katalyse, KU Leuven, Kardinal Mercierlaan 92, B-3001 Heverlee, Belgium

Received April 19, 1996; revised November 1, 1996; accepted December 2, 1996

The mechanism of zeolite Y destruction by steam in the presence of vanadium is described. Electron spin resonance, UV–VIS diffuse reflectance, and sorption measurements are used to understand vanadium dynamics on the zeolite. Vanadium deposited on the external surface of the zeolite migrates into the channels by being heated in oxidizing atmosphere; although water helps vanadium reach the acid sites, it is not required. Vanadium is stabilized as VO_2^+ cation near the acid sites. The strongest acid sites can stabilize V as VO^{2+} cations, but experimental results show that V^{IV} does not play any role in zeolite destruction. Extraframework aluminum competes with the zeolite for vanadium and delays its migration to the acid sites. In the presence of water vanadic acid is formed inside the zeolite according to the reaction VO_2^+–Y + 2 H_2O ⇌ H^+–Y + H_3VO_4. Since vanadic acid is a strong acid, it can destroy the zeolite by hydrolysis of the SiO_2/Al_2O_3 framework; in this way, vanadium can act as a catalyst for zeolite destruction. Synergistic action between sodium and vanadium is explained. A detailed mechanism for zeolite dealumination by steam is proposed. © 1997 Academic Press

INTRODUCTION

Poisoning and deactivation of the catalyst in fluid catalytic cracking (FCC) by vanadium contained in the oil feedstock is one of the most prominent problems faced by operators of oil refineries. The effects of metal contaminants such as vanadium and nickel on the performance of cracking catalysts are well known (1–3). Vanadium and nickel, present in the feed as organic complexes and porphyrins (4), are deposited continuously on the catalyst surface. They promote undesirable dehydrogenation, which increases coke and dry gas production at the expense of the gasoline yield. Vanadium has the additional effect of reducing the catalyst activity and selectivity by destroying zeolite crystallinity.

[1] To whom correspondence should be addressed. E-mail: ctrujill@ciencias.ciencias.unal.edu.co.

Although much work has been done in the field, the mechanism by which zeolite is damaged in the presence of vanadium is still a matter of controversy (3–9). Understanding the mechanism of zeolite destruction by vanadium is very important and helpful in the designing of better vanadium traps. Worsmbecher *et al.* (5) proposed a mechanism for framework collapse in the presence of vanadium. It involves the hydrolysis of the zeolite SiO_2/Al_2O_3 framework by H_3VO_4 produced by the reaction between V_2O_5 and water. An H_3VO_4 equilibrium concentration in the regenerator atmosphere between 1 and 10 ppm was calculated. Since vanadic acid is a strong acid it can attack the Si–O–Al bond by extracting aluminum from the lattice, causing collapse of the structure. After zeolite destruction vanadium pentoxide may combine with rare earth compounds left as debris to form rare earth vanadates.

M. L. Occelli (3, 7) proposed that zeolite is destroyed by $H_4V_2O_7$, according to results on vanadium scavengers forming $Mg_2V_2O_7$. Wormsbecher showed that steam is necessary for vanadium action, and Pine (8) clearly showed that vanadium acts as a catalyst for the steam–zeolite reaction; therefore, vanadium must interact in some way with steam.

The controversy over the acid species formed between V_2O_5 and water was solved by Sanchez and Hager (10). They established that H_3VO_4 is the volatile species formed between V_2O_5 and water at high temperatures. The reaction was found to be

$$V_2O_{5\,(l)} + 3\,H_2O_{(g)} \rightleftharpoons 2\,H_3\,VO_{4(g)}, \qquad [1]$$

ΔG°(cal/mol) = 48,154.1 + 11.435 T ln T − 0.004844 T^2 + 286,850/T − 78.265 T. For a typical FCC regenerator temperature of 993 K, $K_p = 1.772 \times 10^{-10}$.

As an example, a normal vanadium concentration in the feed to a FCC unit is 3 ppm. With this value, around 6% (w/w) of the feed is converted to coke with a hydrogen content of 8% (11). To burn off the coke produced by 1 kg of the feed, using an excess of 2% of air (20% of O_2), it is necessary to inject into the regenerator 29.98 mol of air (11).

0021-9517/97 $25.00
Copyright © 1997 by Academic Press
All rights of reproduction in any form reserved.

The complete combustion increases gases to 30.78 mol with a water content of 7.8% produced by hydrogen burning. There is some water contribution from the stripping zone, which increases the partial pressure of steam to the typical value of 20% (5). Under these conditions the exhaust gases, per kilogram of the feed processed, reach 35.48 mol or 1445 liters at 993 K and 2 atm.

A steam partial pressure of 20% and 2 atm regenerator pressure yields an equilibrium concentration of 3.37×10^{-6} atm or 1.7 ppm of H_3VO_4. To reach the equilibrium it is necessary to volatilize 3.0 mg of vanadium per kilogram of feed processed. This is the same amount contained in 1 kg of the feed considered as an example. Taking into account that the regenerator atmosphere is renewed continuously, if the equilibrium is reached all vanadium would be lost with regenerator exhaust gases. In order to explain the observed vanadium accumulation over the catalyst it is necessary to accept that vanadic acid bulk concentration must be below 1 ppm and not between 1 and 10 ppm as proposed by Wormsbecher.

In the FCC process approximately 5–10% of the sulfur present in the feed is incorporated into the coke and transferred to the regenerator, where it is oxidized to SO_x (90% SO_2, 10% SO_3) (12). A typical feed contains 1% of sulfur (11). Simple calculations will show us that the minimum concentration of SO_3 or sulfuric acid in the regenerator atmosphere would be around 60 ppm. If the mechanism of Y zeolite destruction by vanadium is an acid hydrolysis, it is not clear why it would be caused by the weaker acid in lower concentration and not by the stronger and more abundant sulfuric acid.

Zeolite destruction by vanadium is real, so if the mechanism is an acid hydrolysis as proposed by Wormsbecher, it is necessary the concentration of the vanadium in the zeolite before destruction. To explain the catalytic action of vanadium it would be necessary to concentrate it inside the zeolite; the destruction either is carried out by acid hydrolysis or is caused by liquid V_2O_5 (13).

Other mechanisms have been proposed; for rare earth containing zeolites, it has been shown by high-resolution analytical microscopy that vanadium reacts with lanthanum in LaY zeolite to form $LaVO_4$. The destabilization of the zeolite was attributed to the disappearance of La–O–La stabilizing bridges in the sodalite cages (14, 15). However, the levels of vanadium used to draw out those conclusions were high compared with the values found in equilibrium FCC catalysts and do not agree with the observation that small amounts of vanadium destroy large amounts of zeolite (8). Further experiments have shown that vanadium behaves as a catalyst for zeolite destruction by steam (8). If the formation of rare earth vanadates were the cause of zeolite destruction, vanadium would be a reactant and the amount of vanadium needed for the large activity decays observed would be higher. It has been proposed that VO^{2+} cations play an important role in calcined rare earth Y zeolite (CREY) (3), USY, and rare earth Y zeolite (REY) destruction (8). Anderson *et al.* (18) first concluded that when a Eu–Y zeolite is loaded with vanadyl naphthenate, octahedral coordinated VO^{2+} cations are stabilized on the zeolite after organic ligand combustion.

Kinetic measurements of the zeolite destruction in the presence and absence of vanadium and sodium were made by Pine (8). The results show steam as a reactant in zeolite destruction and vanadium and sodium as nearly equally active, synergistic catalysts. Rare earth elements do not change zeolite vanadium tolerance. Their effect is indirect; they change the base steam stability of the zeolite. Pine proposed that the reaction of hydroxyl groups with the weak bases sodium and vanadium would have a destabilizing effect on the adjacent Si–O–Si bond and make them more amenable to hydrolysis by steam. Occelli showed that vanadium tolerance decreases by increasing framework aluminum content, indicating that the point of attack could be the Si–O–Al bond (6). X-ray diffraction shows that the zeolite is transformed by heating to a more stable phase like mullite and cristoballite; with vanadium this transformation occurs at lower temperatures (3). Occelli found that steam accelerates and enhances the deleterious effects of V; it was proposed that the damage to the catalyst occurs during the stripping in the FCC cycle by vanadium volatile acids, which can react with the catalyst components (3). However, it is unlikely to find V^V after the strong reducing conditions of the cracking reaction and steam-stripping and there are no known volatile vanadium acids in lower oxidation states.

Data from imaging secondary-ion mass spectroscopy show that vanadium accumulates throughout FCC catalyst particles, but shows a preference for rare-earth-exchanged zeolite Y and alumina phases in a composite catalyst (16). Torrealba *et al.* (17) studied the effects of 1% vanadium impregnation on an ultrastable zeolite (USY) and one FCC catalyst. The vanadium is well dispersed on the zeolite either by calcination at 540°C or by hydrothermal treatment at 750°C. In the FCC catalyst vanadium is present as large aggregates (6 to 12 nm). Vanadium decreases the stability and consequently the activity of the zeolite and FCC catalyst by increasing the rates of dealumination during the hydrothermal treatment. However, the loss in zeolite crystallinity alone was insufficient to explain the high activity decay. Ion exchange of acid protons by cationic vanadium species seems responsible for activity loss in the remaining USY crystals (17).

In order to clarify the zeolite destruction mechanism by steam in the presence of vanadium, in this research we use electron spin resonance (ESR) to quantify the role of V^{IV} in the vanadium–Y zeolite interaction. Diffuse reflectance spectroscopy (DRS) in the UV–VIS region and sorption measurements are used in combination with ESR to explain V behavior in the zeolite. The effects regarding support

type, temperature, and atmosphere (dry–steam, oxidative–reductive) over V speciation are investigated. The different aspects such as crystallinity loss by lattice destruction and activity decrease are discussed.

EXPERIMENTAL

For this study two zeolite samples from PQ Corporation were selected: references CBV600 and CBV712, henceforth referred to as Z6 and Z7, respectively. Z6 is a normal USY with extraframework aluminum (EFAL), bulk Si/Al ratio 2.76, unit cell size (A_o) 24.38 Å, Na_2O 0.18%. Z7 is produced by acid extraction of Z6 and contains lower levels of EFAL, bulk Si/Al ratio 5.45, A_o 24.32 Å, Na_2O 0.08%. The zeolites were kept in a saturated $CaCl_2$ solution to stabilize water content. The total water content was determined by weight loss after calcination at 1000°C.

Aerosil 200 (Degussa) and alumina were used for comparison. As aerosil is too light to be manipulated into the quartz flow cell, handling could be improved by wetting 25 g with 250 ml of water and drying at 120°C overnight. The dried product was ground in a small agate ball mill. The resultant silica has no important changes in surface area (Table 2). Alumina was prepared by calcination of iron free pseudobohemite at 750°C. Gases were supplied by L'Air Liquid: compressed air, N_2 99.9%, and CO 12.5% in N_2.

Vanadium was added using a variation of the procedure published by Mitchell (39) and similar to that used by Pine (8). We choose bis[1-phenylbutandionato-(1,3)]-oxovanadium (IV) (vanadyl bisbenzoilacetonate (VBzA) from Merck) to simulate vanadium deposition under FCC conditions. The main part of V compounds in the crude oil exists as metal porphyrin or porphyrin-like complexes (4). These molecules are larger than the Y zeolite mouth pores and when deposited on FCC catalyst the metal can not enter directly into the zeolite. The Mitchell procedure uses vanadium naphthenates that are commercially more available than porphyrines. Naphthenates are made from naphthenic acids with a general formula written as $R(CH_2)_n \cdot COOH$, where R is a cyclic nucleus composed of one or more rings (1). Commercial vanadium naphthenates are an irreproducible mixture of different molecular weights and sizes, and the smallest members can enter Y zeolite pores during the Mitchell procedure. From the data published by Hong *et al.* (41), VBzA was modeled and it was concluded that there is not an orientation that let the molecule enter Y zeolite pores.

VBzA dissolved in toluene was added to the fully hydrated supports. Toluene is less polar than methanol (used by Pine) and for the size of VBzA and the polarity of the solvent the vanadium is deposited on the external surface of the zeolites during impregnation, simulating FCC deposition. The solvent was evaporated in a rotavap under vacuum. The resulting product was calcined in a vertical quartz tube, heated at 2°C/min up to 300°C for 5 h in an oxygen stream. Oxygen atmosphere and a calcination temperature lower than that used by Mitchell (air, 537°C) were chosen in order to eliminate organic ligands keeping vanadium on zeolite's external surface. VBzA oxidizes very easily under these conditions, probably due to the catalytic action of V for organic matter oxidation. Samples precalcined at 300°C in oxygen were calcined at higher temperatures in shallow dishes in a muffle oven in air for 5 h unless a different period is specified. The heating rate was 2°C/min.

Steaming of the zeolites was performed in a vertically mounted quartz tube 3.0 cm in diameter, provided with a sintered quartz plate. The lower part of the tube was connected to a stainless steel (ss) T provided with a septum. Water was pumped by a syringe perfusor, in which a needle passes through the septum and discharges water into the heated part of the tube. In this way liquid water accumulation and condensation were avoided. The upper part of the tube was welded to a Pyrex screw. A Teflon male screw with an O-ring was placed between the reactor and a Pyrex tube 2.6 cm in. diameter connected to a ss T. The thermocouple was covered by a 3-mm quartz tube and inserted into the upper T and sealed by Swagelock fittings. A nylon pipe connected to the ss T introduced gases into the lower part of the reactor, gas flow rates were measured by flowmeters. The atmosphere during steaming was 90% water, 10% gas unless a different proportion is specified; 4.0 ml/h and 10 ml/min (293 K), respectively. The heating rate was 5°C/min in a flow of the corresponding gas. Water was added after treatment temperature was reached and time measured from this point. The gases leaving the tube were conducted via a hose through the condenser. Steaming, in the presence of ammonia, was done with a solution of 0.56 *M* NH_4OH and N_2, obtaining an atmosphere of 90% water, 1% NH_3, and 9% N_2.

To prepare zeolite samples with vanadium located mainly on the internal surface, H-USY zeolites were exchanged with vanadium. VO^{2+}-USY zeolites were prepared by ion exchange with aqueous solutions of $VOSO_4$ (Acros). Henceforth impregnated samples will be referred as "imp."and exchanged zeolites as "exc." Samples Z6 exc. 0.82%V and Z7 exc. 0.70%V were prepared by stirring 10.0 g (dry) of the zeolite in 250 ml of 0.01 *M* $VOSO_4$ aqueous solution over 24 h. Sample Z7 exc. 3.9%V was prepared by stirring 5.0 g (dry) of Z7 in 200 ml 0.10 *M* $VOSO_4$ for 1 week. To avoid oxidation the exchange was performed under a N_2 atmosphere. After the exchange, samples were centrifuged and washed three times with deionized water. To eliminate water excess, zeolites were stirred in ethanol and then in acetone. The acetone was vacuum evaporated and the samples were allowed to rehydrate over saturated $CaCl_2$ solution. Vanadium was analyzed after dissolving the hydrated zeolite with HF in

platinum crucibles. Sulfuric acid was added to the solution and HF evaporated. Vanadium was reduced by sodium sulfite and the excess SO_2 was boiled off and the solution titrated with a standardized solution of $KMnO_4$ 0.010 *N*. Control samples were also used.

The ESR measurements were collected on a Bruker ESP 300E, operated at the X band (9.58 GHz) and calibrated against DPPH. A quartz tube of 2.3 mm internal diameter was used as a cell. To perform quantitative measurements, the ESR signal intensity needs to be proportional to the V^{IV} mass; it was obtained when the sample height in the tube was 1 cm centered in the cavity. The best method of comparing signal intensities was to use the height of the large central peak in the spectrum ($g = 2.04$). It is less sensitive to base line distortion due to iron impurity interference. This distortion introduces large uncertainties in the numerical double signal integration, especially for low V^{IV} containing samples. The sample weight was determined with approximation to the 0.1 mg; the signal intensities were normalized to 20.0 mg and gain 1×10^5 by spectra multiplication with factor *f*, where $f =$ (20.0/mass of the sample) $\times$ (1×10^5/gain used to collect the spectrum).

The spectra were collected at 150 K, modulation frequency 100 kHz, modulation amplitude 10 G, time constant 0.64 ms, resolution of the field axis 2048 points, sweep time 83.89 s, microwave power 0.020 W. When the microwave power was changed comparisons were made keeping in mind that the intensity of an ESR signal increases proportionally to the square root of the microwave power if the signal is not saturated. No saturation of the signal was observed under working conditions. A calibration curve was made with frozen aqueous solutions of vanadyl oxalate prepared by reduction of V_2O_5 99.9% (Acros) with oxalic acid (Merck). An excellent linearity between the signal intensity and vanadium mass (Fig. 2) was found for solutions with 20 to 200 ppm of V, when a mass of around 50 mg of solution was used in the cell.

UV–VIS DRS spectra were collected on a Varian Cary 5 spectrophotometer with DRS attachment. The spectra were taken in the 200- to 800-nm range using the corresponding solid, without vanadium, treated in the same way as the sample as blank.

To check O_2 and atmospheric moisture interference in ESR, DRS spectra, and signal intensities, some samples were calcined in a quartz flow cell with Suprasil window for DRS and side arm for ESR. It was determined that the small amount of water adsorbed during manipulation and recording of the spectra in an open cell does not affect the DRS and ESR V/zeolite and V/alumina spectra. However, the V/silica DRS spectrum is quite sensitive to moisture as previously reported (19). In accordance with Huang *et al.* (20), we did not observe interference of the atmospheric oxygen in the system VO^{2+}–Y zeolite. Zeolites and alumina spectra were recorded in open cells and silica spectra in the quartz flow cell.

Adsorption measurements were performed in an Omnisorp 100 system from Coulter. Before adsorption the samples were heated to 400°C under vacuum (10^{-3} Pa) for at least 5 h. The multipoint BET surface area was calculated between $0.05 < P/P^\circ < 0.25$. The micropore volume was obtained from a T-plot analysis (thickness T-layer among 2 and 9 Å) as proposed by Lippens and de Boer (21).

RESULTS

Electron Spin Resonance Spectroscopy

The ESR spectra of the CBV712 (Z7) impregnated with 0.4%V calcined at 500°C and the vanadyl ion in aqueous solution are compared in Fig. 1. V^{IV} in the zeolite presents a hyperfine structure characteristic of isolated (not interacting) vanadyl ions. However, the $g_\perp$ tensor is not as well resolved as it is in frozen aqueous solution. A complete ESR study of vanadium introduced in Y zeolite by calcination may be found elsewhere (20). Huang *et al.* (20) found two different positions for vanadyl species in Y zeolite, one

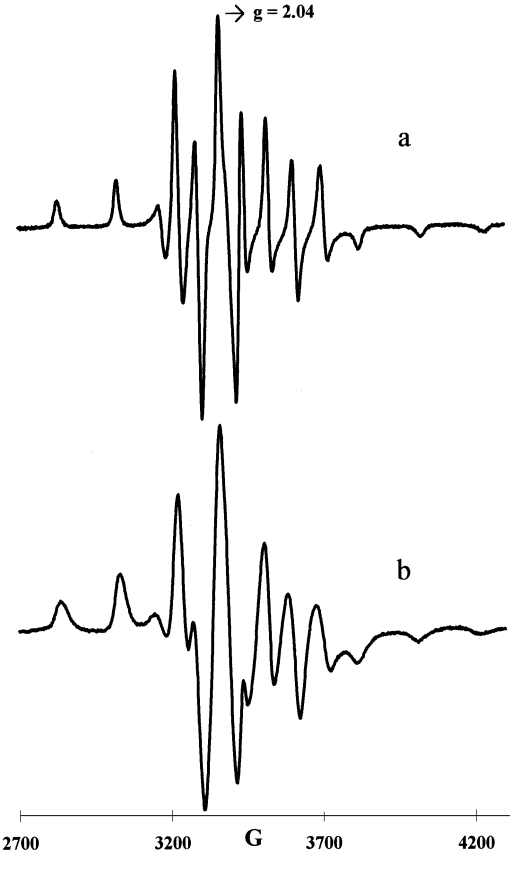

FIG. 1. ESR spectra of (a) aqueous vanadyl ion, (b) Z7 imp. 0.4%V calcined at 500°C.

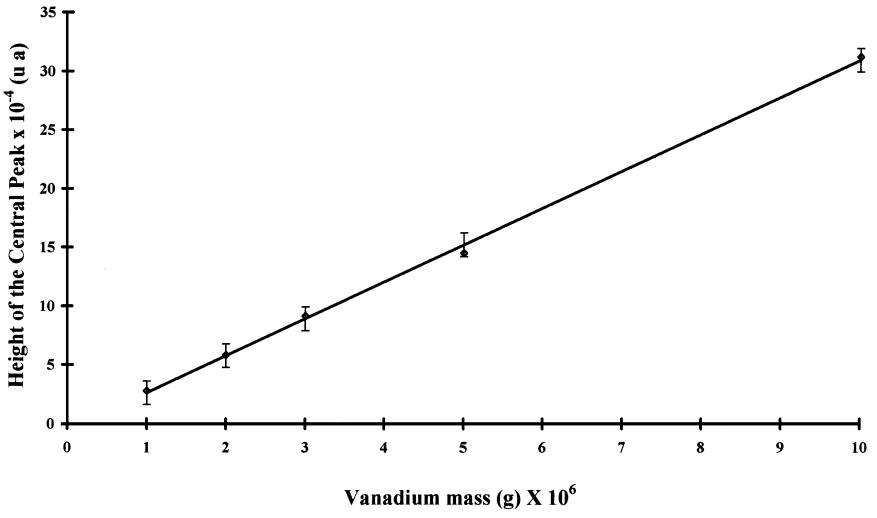

FIG. 2. Calibration curve. ESR signal intensity versus vanadium mass.

in the supercage and another probably in the β-cage. For both positions, the vanadium has a distorted tetrahedral or a pyramidic coordinated symetry.

The calibration curve made with frozen aqueous solutions of vanadyl oxalate is shown in Fig. 2. It is worth showing that ESR is a very sensitive technique detecting and quantifying amounts of V^{IV} below 1×10^{-6} g. Table 1 presents the percentage of V^{IV} on the total vanadium (V_T) for all samples as a function of temperature of calcination in the specified atmosphere.

For impregnated zeolites the percentage of V^{IV} in the total vanadium content (V_T) is shown in Fig. 3. The samples calcined at 300°C contain between 1 and 2% of V_T as V^{IV}.

TABLE 1

Percentage of V^{IV} on the Total Vanadium (V_T) Content for Impregnated or Exchanged Samples as a Function of Calcination Temperature in the Specified Atmosphere

Sample	$\%V^{IV}/V_T$				
	300°C	400°C	500°C	600°C	700°C
Z6 imp. 0.2%V, air	1.19	1.13	1.25	1.45	1.66
Z6 imp. 0.4%V, air	0.87	0.90	1.49	1.67	1.23
Z7 imp. 0.2%V, air	1.93	4.34	5.35	4.30	2.10
Z7 imp. 0.4%V, air	1.48	2.70	4.21	2.61	1.51
Z7 imp. 0.2%V, air, 72 h			4.60		
Z6 imp. 0.2%V, 20% H_2O/air			2.84		1.34
Z6 imp. 0.4%V, 20% H_2O/air			2.17		1.01
Z7 imp. 0.2%V, 20% H_2O/air			6.75		2.87
Z7 imp. 0.4%V, 20% H_2O/air			8.25		2.35
Z6 exc. 0.82%V, air	7.97	10.11	13.98	9.21	5.26
Z7 exc. 0.70%V, air	9.97	9.88	14.93	9.74	4.37
Silica 0.4%V, air	1.33	0.75	dbnq	dbnq	dbnq
Alumina 0.2%V, air	0.87	dnbq	dnbq	dnbq	dnbq

Note. dbnq, detectable but not quantifyable.

It is clear that, at this temperature in oxygen atmosphere, organic ligands have disappeared, at this stage the color of the samples is yellow-brown, indicating that most of the vanadium is present as V^V, ESR inactive. Further calcination of the zeolite in air produces color changes and variations in V^{IV} concentration. In Z7 samples amazingly the proportion of V^{IV} increases with temperature despite the heating made in the oxidizing atmosphere. The proportion of V^{IV} for Z7 imp. 0.2%V reaches a maximum of 5.35% at 500°C. At 700°C, V^{IV} content is almost the same as at 300°C. In CVB600 (Z6) impregnated zeolites, V^{IV} concentration stays almost constant in the range of temperatures studied when calcination is made in air.

In order to check whether 5 h was long enough to establish the equilibrium between both oxidation states in the zeolite, Z7 imp. 0.2%V was calcined at 500°C for 3 days. The result shows (Table 1) that 5 h is enough time and the amount of V^{IV} has a tendency to decrease (instead of increase) with heating time. To check the effects of water on V^{IV}–V^V equilibrium, samples of Z6 and Z7 impregnated with 0.2 and 0.4%V were calcined in the presence of 20% water at 500 and 700°C for 5 h. Results are shown in Table 1. At 500°C all samples show an increase in V^{IV} content, indicating that water helps vanadium to reach the sites where it can be stabilized as V^{IV}. At 700°C the proportion of V^{IV} is higher in Z7 imp. samples treated with 20% of steam than in the samples calcined at the same temperature in air; however, Z6 imp. samples contain even lower levels of V^{IV} than the corresponding samples treated in air. Water plays a role in vanadium displacement but does not seem to affect directly V^V–V^{IV} equilibrium.

To check the ability of zeolite Y to stabilize V^{IV} in oxidizing atmospheres, exchanged zeolites, Z6 exc. 0.82%V and Z7 exc. 0.70%V, were calcined in the same way as impregnated samples. The results presented in Table 1 and Fig. 4

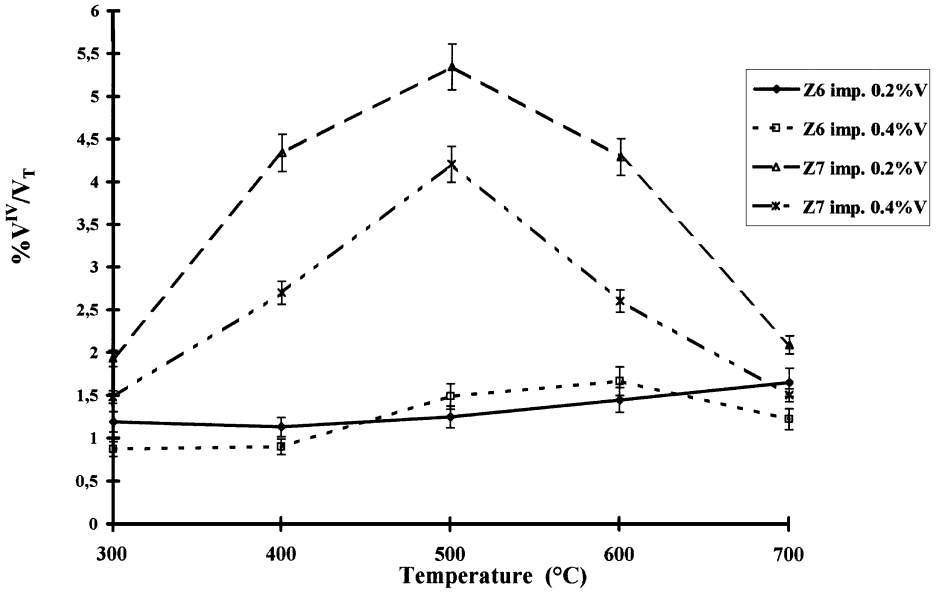

FIG. 3. Percentage of vanadium IV on the total vanadium in the sample as a function of temperature of calcination for impregnated zeolites.

indicate that at 300°C more than 90% of the original V^{IV} has been oxidized. The shapes of the curves in Fig. 4 are similar to those of the Z7 imp. samples in Fig. 3. Amazingly with heating in air at temperatures higher than 300°C a reduction of vanadium is observed until 500°C, and after this temperature V^{IV} is oxidized again. Although the proportions of V^{IV} with temperature are higher for exchanged than for impregnated zeolites, these results show that zeolite Y can stabilize vanadium as V^{IV} but it is just a fraction that depends on temperature. At the normal temperatures present in the regenerator of a FCC unit (720°C), most of the vanadium on the zeolite must exist as V^{V}.

During the treatment previous to adsorption measurements, it was observed that vanadium containing zeolites changes its color from white to gray-black. This color change indicates V^{V} reduction. Figure 5 presents the ESR spectra of the sample Z7 imp. 0.4%V calcined to 700°C and evacuated on heating at 450°C for 8 h. It can be seen

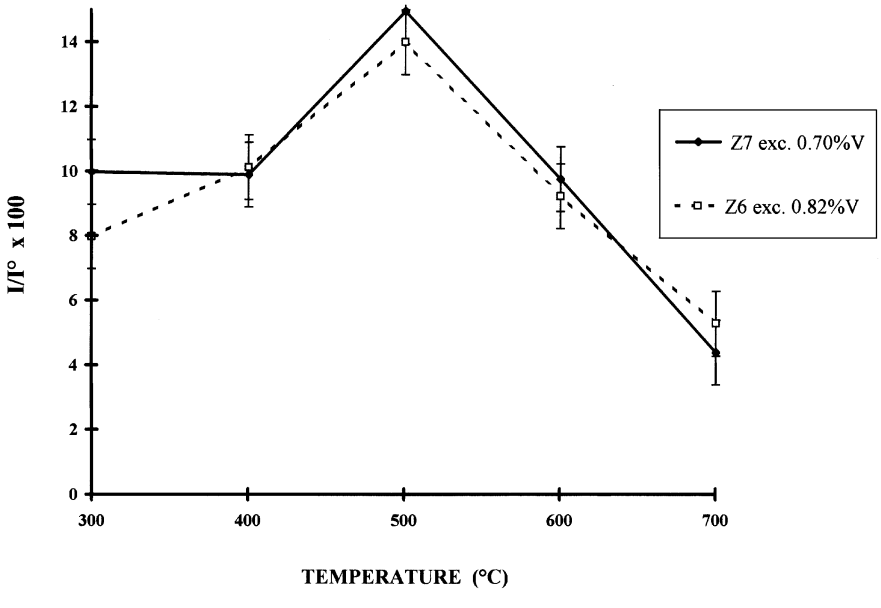

FIG. 4. Percentage of the ESR signal intensity *I* remaining after calcination of exchanged zeolites as a function of temperature. I° is the ESR signal intensity of the fresh exchanged solid.

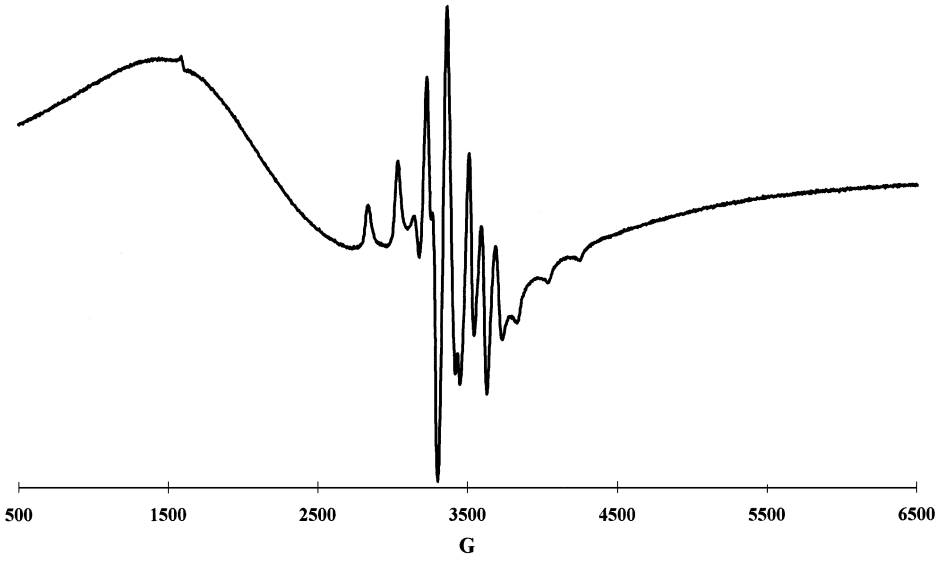

FIG. 5. ESR spectra of Z7 imp. 0.4%V calcined in air at 700°C and then evacuated at 450°C, 10^{-3} Pa for 8 h.

that the ESR signal of the isolated vanadyl ion is now superimposed on a very broad signal assigned to amorphous dispersed V_2O_4. The small peak at the low field superimposed on the broad signal is due to iron impurity present in the sample.

UV–VIS Diffuse Reflectance Spectroscopy

Charge-transfer spectra of vanadium containing samples were recorded in the region 200–800 nm using identically treated supports without vanadium as reference. In the case of pure compounds $BaSO_4$ was the reference. The oxygen → vanadium charge-transfer absorption band, which is correlated with the minimum diffuse reflectance, is strongly influenced by the number of ligands surrounding the central vanadium ion and thus provides information on its coordination.

Figures 6 and 7 show the DRS spectra of Z6 imp. 0.2%V and Z7 imp. 0.2%V calcined at 300, 500, and 700°C. The spectra correspond with the observed color of the samples. The impregnated zeolites calcined at 300°C are brown-yellow; as the calcination temperature increases the color loses intensity and at 500°C the samples are almost white. The DRS spectra of impregnated zeolites calcined at 300°C show an intense absorption between 800 and 375 nm. This absorption is strongly reduced and completely disappears in the samples calcined at 500 and 700°C, respectively. In the UV region the spectra show two peaks: (1) between 212 and 209 nm and (2) between 266 and 258 nm. The higher the calcination temperature, the higher the energy of the absorption, for samples calcined at 300°C, peak 1 appears at 212 nm and peak 2 at 266 nm, while for samples calcined at 700°C, peak 1 appears at 209 nm and peak 2 at 258 nm.

The DRS spectra of fresh and calcined samples of Z6 exc. 0.82%V and Z7 exc. 0.70%V are shown in Figs. 8 and 9. The freshly exchanged solids are pale blue. The spectra

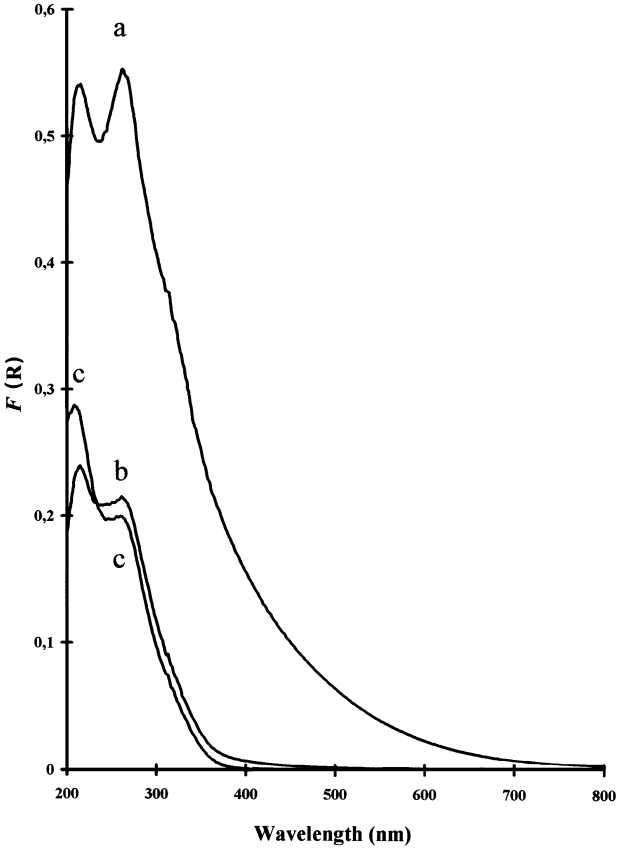

FIG. 6. DRS spectra of Z6 imp. 0.2%V calcined at (a) 300°C, (b) 500°C, and (c) 700°C.

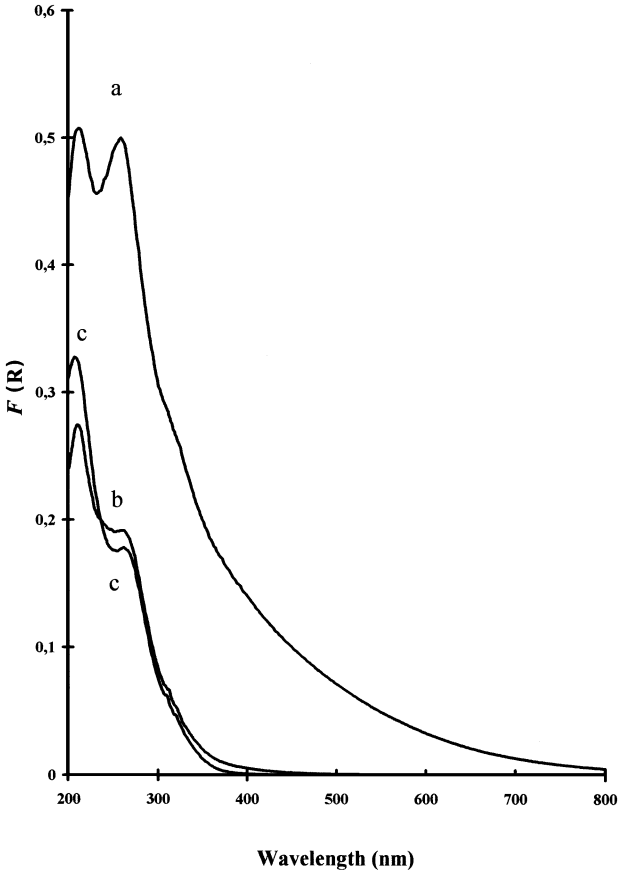

FIG. 7. DRS spectra of Z7 imp. 0.2%V calcined at (a) 300°C, (b) 500°C, and (c) 700°C.

show a very broad and weak band centered at 750 nm assigned to vanadyl d–d transitions (22). The features in the UV region are similar, but less intense compared to those found in the calcined samples. Calcination of the exchanged zeolites at 300°C produces brown solids with strong absorption over the whole range of the visible region and an increase of the absorption in the UV region. At this temperature Z6 exc. 0.82%V spectrum presents two well-defined peaks at 219 and 267 nm and Z7 exc. 0.70%V peaked at 212 and 258 nm. Calcination at higher temperatures reduces the absorption in the visible region in the same way as impregnated samples. The samples calcined at 500°C are pale beige in color and at higher temperatures they are white.

The lowest UV absorption is shown by the freshly exchanged samples. For calcined samples of exchanged and impregnated zeolites the highest reflectance is found at 500°C. This value coincides with the temperature at which the maximum amount of V^{IV} was found in Z7 impregnated and Z6 and Z7 exchanged samples after calcination. This implies that although the molar absorptivity of V^{IV} in the zeolite is smaller than V^{V}, it is not easy to differentiate between the two oxidation states from the UV absorption.

To compare with vanadium on the zeolites, Figs. 10 and 11, shown the DRS spectra of anhydrous samples of vanadium 0.2% on silica and alumina calcined at 300, 500, and 700°C. In these cases the lowest absorption is found at 700°C. At 300°C samples are orange. As the temperature increases, vanadium on silica in anhydrous conditions becomes white, while on alumina it keeps the pale beige color even on calcination at 700°C. At 700°C, vanadium on silica shows three peaks: a weak shoulder around 300 nm, the main peak at 246 nm, and third one at 219 nm. Vanadium on alumina clearly behaves in a different way, at 700°C a single broad absorption band is seen at 287 nm.

For comparison DRS spectra of different vanadium compounds are given in Fig. 12. $VOSO_4xH_2O$ has an octahedral V^{IV} coordination and absence of V–O–V bonds; its d–d transition band appears at 747 nm (22, 33) and two bands in the UV at 218 and 267 nm are seen. Similar bands in the UV region, at 218 and 285 nm, are shown by polymeric tetrahedral V^{V} in NH_4VO_3, where no V=O bonds are present. Polymeric distorted trigonal bypiramids of VO_5 in V_2O_5 show similar bands at 224 and 256 nm. Bands due to polymeric vanadium are located between 300 and 500 nm in accordance with previous studies (24, 25). The three

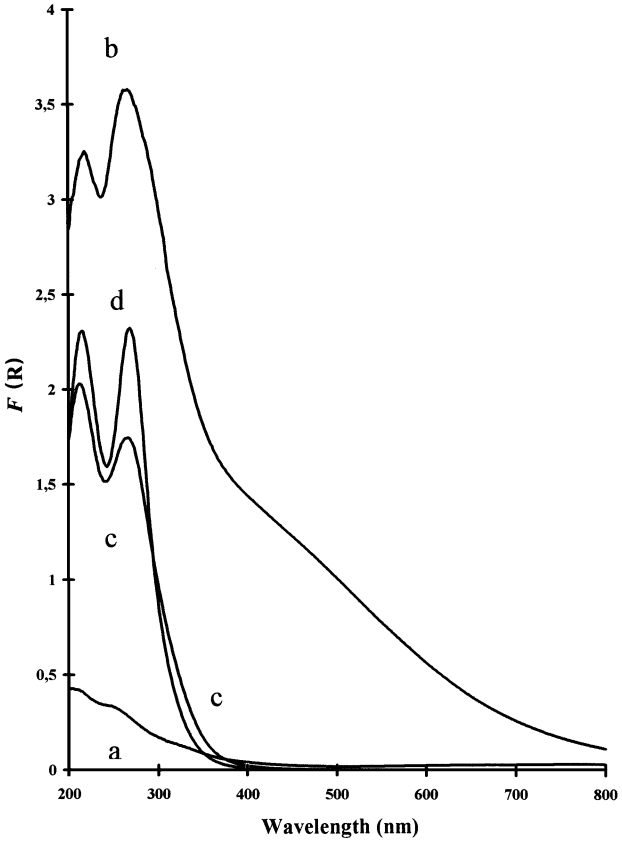

FIG. 8. DRS spectra of Z6 exc. 0.82%V (a) fresh and calcined at (b) 300°C, (c) 500°C, and (d) 700°C.

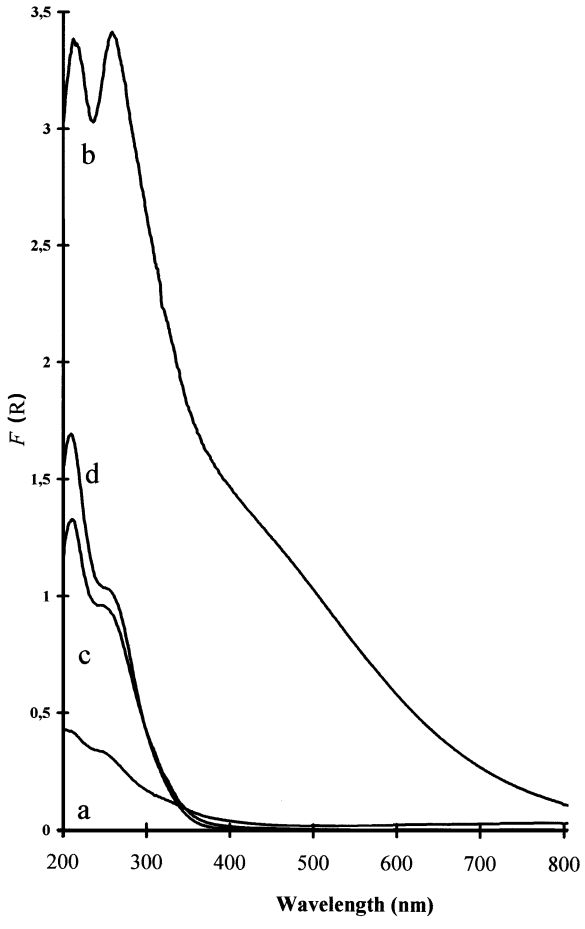

FIG. 9. DRS spectra of Z7 exc. 0.70%V (a) fresh and calcined at (b) 300°C, (c) 500°C, and (d) 700°C.

vanadium compounds in Fig. 12 display two bands between 200 and 300 nm, due to charge transfer transitions of the V−O bond allowed in the three compounds studied. Contrary to suggestions before (24, 26) it is not possible to differentiate between V^{IV} and V^{V} for the absorption in the UV region.

The effects of evacuation at 450°C after calcination at 700°C for the Z6 and Z7 imp. 0.4%V samples on the DRS spectra are shown in Fig. 13. The evacuation of the calcined samples produces color changes from white to gray-black; the color intensity for the same level of vanadium is higher in Z7 than in Z6 zeolite. The spectra show a strong d–d transition absorption in the visible region due to V^{IV} formed during the evacuation. From Fig. 13 is clear that the amount of V^{V} reduced is greater in Z7 than in Z6 under the same conditions.

Adsorption Measurements

The results obtained by adsorption measurements on different samples are shown in Table 2. The remaining crystallinity %*C*/C° is determined by the quotient between the micropore volume in the sample and the micropore volume in the as-received untreated zeolite without vanadium. The result shows that Z7 has a larger micropore volume than Z6, as expected due to EFAL presence in Z6. The calcination in air at 700°C of the impregnated zeolites at vanadium levels similar to those present in FCC catalysts does not appreciably affect the crystallinity of the zeolites. This result confirms that steam is necessary for zeolite destruction (5, 8). The steaming of 1%V imp. zeolites in 90% H_2O, 10% air causes the destruction of the zeolite with the consequent reduction in micropore volume; the damage is higher in Z7 than in Z6. These results indicate that EFAL reduces the vanadium action in the zeolite as previously published (3, 13).

The sample Z7 exc. 3.9%V freshly exchanged shows an apparent crystallinity loss of 4.9%; this is due to the fact that no corrections were made for vanadium volume and mass in the micropore volume determinations. Given the small amounts of vanadium used in most samples and the large micropore volume decays after treatments, the correction was considered unnecessary and the data are reported as obtained.

To evaluate the role played by V^{IV} in lattice attack, Z7 imp. 1%V precalcined to 300°C in air (vanadium located

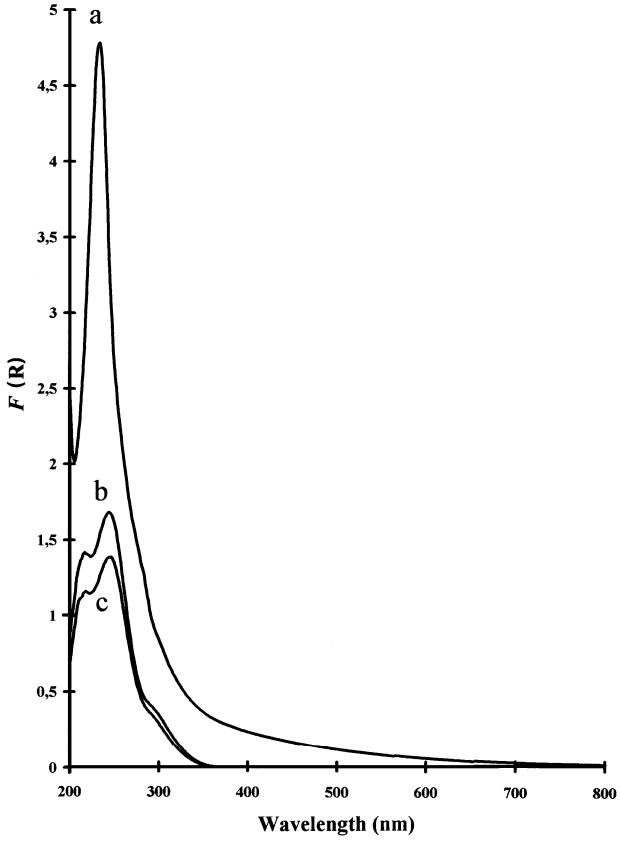

FIG. 10. DRS spectra of 0.2%V on silica calcined at (a) 300°C, (b) 500°C, and (c) 700°C.

TABLE 2

Adsorption Results on the Fresh and Treated Samples

Sample	BET area (m^2/g)	Micropore volume (ml/g)	%*C*/C°
Aerosil fresh	190.5	0	
Aerosil wetted and dried	186.0	0	
Alumina	179.6	0	
Z6 (as received without vanadium)		0.2252	100
Z6 imp. 1% V, 720°C, steam and air, 16 h		0.1314	58.4
Z7 (as received without vanadium)		0.2549	100
Z7, 720°C, steam and air, 16 h		0.2094	82.2
Z7 imp. 0.4% V, calc. 700°C, air, 5 h		0.2547	99.9
Z7 imp. 1% V, 720°C, air, 16 h		0.2376	93.2
Z7 imp. 1% V, 720°C, steam and air, 16 h		0.1211	47.5
Z7 imp. 1% V, 720°C, steam and CO/N_2, 16 h		0.2068	81.1
Z7 exc. 3.9% V, fresh		0.2424	95.1
Z7 exc. 3.9% V, 720°C, steam and air, 16 h		0	0
Z7 exc. 3.9% V, 720°C, steam and CO/N_2, 16 h		0.2070	81.2
Z7, 720°C, steam and NH_3, N_2, 16 h		0.2022	79.3

Note. The remaining crystallinity %*C*/C° is determined by the quotient between the micropore volume in the sample and the micropore volume in the untreated (as received) zeolite without vanadium. For details refer to the text.

on the external surface of the zeolite) was steamed with 90% water 10% a mixture of CO 12.5% in N_2. The destruction of the zeolite was similar to the damage experienced by pure Z7 steamed with 90% water, 10% air. Z7 exc. 3.9% V was treated in the same way; in this case vanadium is located near the acid sites in the zeolite. The structural collapse was again similar to Z7 steamed in 90% water, 10% air without vanadium. When Z7 exc. 3.9% V was steamed in 90% steam, 10% air, framework collapse was complete. This is a real proof that vanadium must be present as V^V to catalyze zeolite destruction.

When Z7 was steamed in the presence of ammonia the lattice damage was of the same order as in the sample treated in the absence of ammonia. This result and the results obtained by steaming Z7 in the presence of V^{IV} indicate that weak bases do not accelerate framework hydrolysis.

DISCUSSION

Solid ion exchange between HY and vanadium pentoxide has been studied by Huang *et al.* (20). Their results show that vanadium enters into the channels and it is stabilized as V^{IV} and V^V near the acid sites. Kucherov and Slinkin introduced V, Cu, Cr, and Mo into H-ZSM-5 and H-mordenite by zeolite calcination with metal oxides at temperatures ranging from 520 to 820°C. Their results show that ions migrate from the outer surface of the zeolite crystal and are coordinated in the cationic positions of the zeolites. They also found that acid sites in zeolites act as powerful traps for migrating ions and that the stabilization of V^{IV} requires acid sites stronger than those present in H-(Ga)ZSM-5 (27–30).

From the method used here for impregnation, vanadium is located on the outer surface of the zeolite. This is due to the vanadyl complex with the large organic ligand and the polarity of the solvent. ESR results shown in Fig. 3 indicate that in Z7 imp. samples vanadium migrates from the outer surface, where it is located at 300°C, to the acid sites, where it can be stabilized as VO^{2+}. According to Kucherov and Slinkin (30), the strongest acid sites obligate V^V to autoreduce. V_2O_5 has amphoteric behavior but its character is more acid than basic, while V_2O_4 is more basic than acid, and it is known that V^{IV} and V^V coexist in an equilibrium (40):

$$2\,V_2O_5 \rightleftharpoons 2\,V_2O_4 + O_2. \qquad [2]$$

In an acid–base reaction with a strong acid site V^{IV} will be thermodynamically favored.

ESR results show that V enters into the channels at temperatures as low as 500°C, the displacement of vanadium on the surface does not require steam, and although water

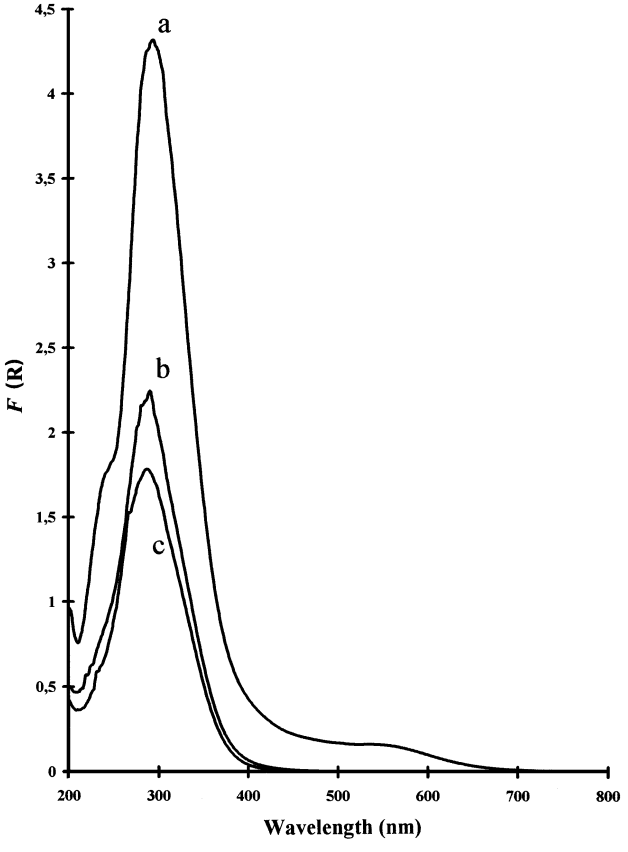

FIG. 11. DRS spectra of 0.2% V on alumina calcined at (a) 300°C, (b) 500°C, and (c) 700°C.

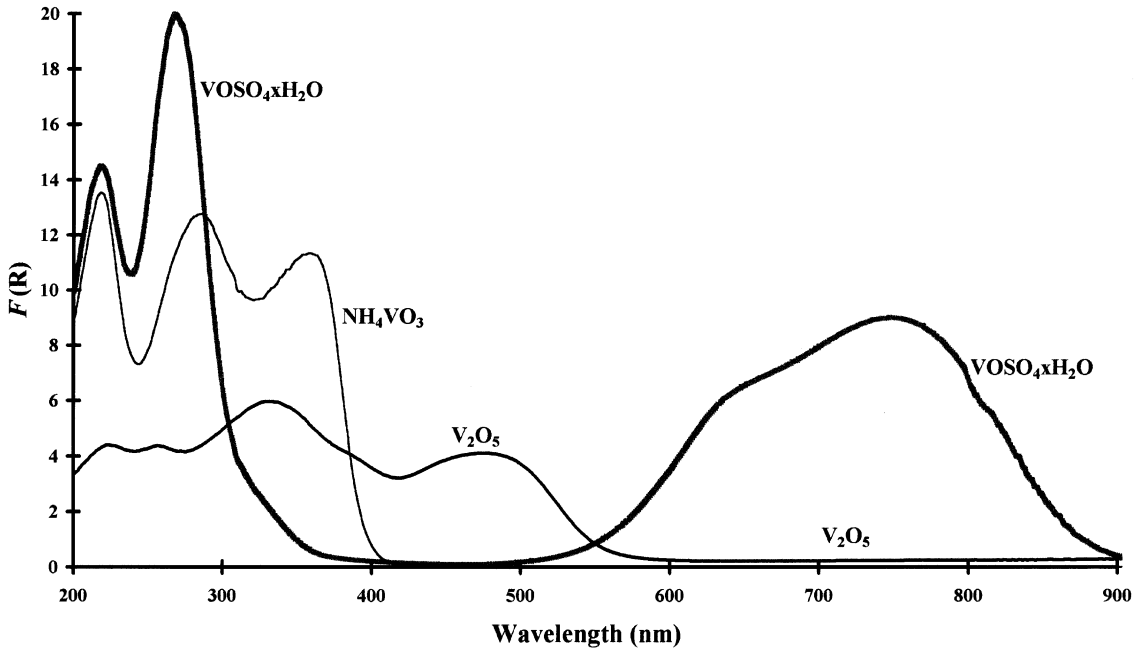

FIG. 12. DRS spectra of some pure vanadium compounds.

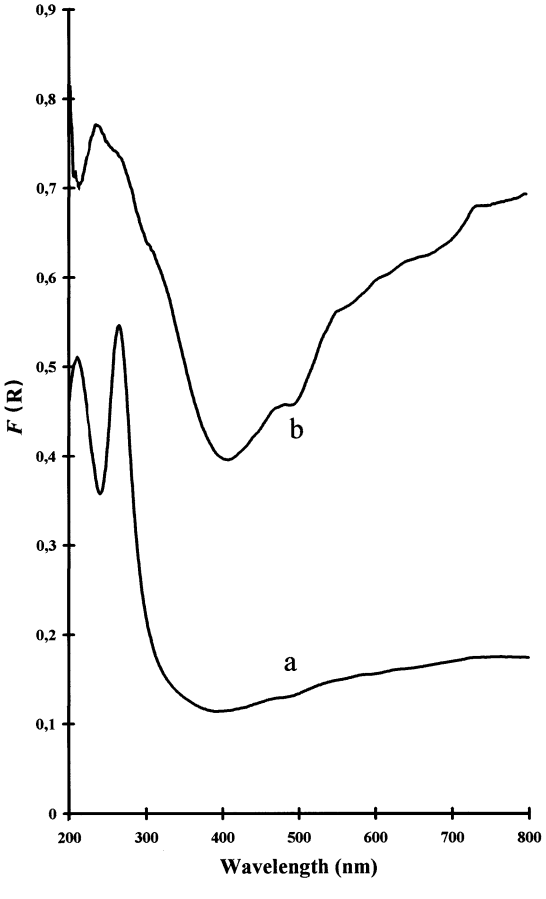

FIG. 13. DRS spectra of Z6 imp. 0.4%V (a) and Z7 imp. 0.4%V (b), calcined to 700°C and then evacuated at 450°C, 10^{-3} Pa.

helps in the migration it is not indispensable. After 500°C the number of acid sites that can keep vanadium as V^{IV} diminishes appreciably. For vanadium on silica and alumina, ESR signals decrease with the temperature of calcination until values are just detectable. Silica and alumina do not have the necessary cationic exchange capacity to stabilize V as V^{IV} in oxidizing conditions.

The differences in vanadium behavior on Z6 and Z7 samples (Fig. 3) must be due to EFAL presence in Z6. EFAL seems to avoid or delay vanadium migration and competes with the zeolite for it. EFAL can act in two ways; complexing vanadium diminishing its mobility, or neutralizing the sites where V can be stabilized as V^{IV} with aluminum cationic species. The reduction of vanadium observed in Z6 imp. 0.4%V by heating in vacuum (Fig. 13) allows us to conclude that both phenomena are present. Vanadium is complexed by EFAL and delays its migration; additionally, the strong acid sites where vanadium can be stabilized as V^{IV} are occupied by aluminum species not present in Z7. As has been pointed out before (3, 13) and confirmed by our experiments, EFAL increases zeolite resistance to vanadium action. It is known that $AlVO_4$ is not a stable compound under FCC conditions (13); thus vanadium cannot be completely immobilized by alumina. Water seems to facilitate vanadium displacement breaking of V–O–Al bridges, allowing it to reach acid sites. This would explain the increase in the ESR signal observed when Z6 and Z7 impregnated samples were treated in 20% steam at 500°C (Table 1). At 700°C in 20% water V^{IV} proportion increases for Z7 samples but decreases

for Z6 samples, which indicates that water also facilitates EFAL movement, and allows it to compete with vanadium for acid site neutralization, protecting in this way the zeolite.

Comparison between Figs. 3 and 4 shows that vanadium-impregnated and -exchanged Z7 samples behave analogous on calcination. This behavior is confirmed by DRS; however, impregnated and exchanged Z6 samples present differences assigned to Z6 higher EFAL content. In Z6 imp. aluminum species must neutralize the acid sites where V can be stabilized as V^{IV}, while during exchange in water solution vanadyl ions can replace them.

The results shown in Figs. 3, 4, 5, and 13 indicate that in Y zeolite there are acid sites with the strength necessary to move the equilibrium of Eq. [2] to the right in air at relatively low temperatures. Without zeolite this reaction moves to the right in air at temperatures higher than 700°C (40). Y zeolites stabilize V^{IV}as VO^{2+}–Y species.

In addition to V^{IV}, V is stabilized as V^{V} near the acid sites. This is demonstrated by the reduction observed on vacuum-heated samples (Fig. 5). Reduction of V^{V} on zeolites by heating has been previously observed (20, 26, 28). The same phenomenon has been observed on iron III-exchanged zeolites (31, 32). Reduction of vanadium (at 450°C, 10^{-9} Pa) could not be observed when alumina or silica are the support.

Support, Atmosphere, and Temperature Effects on Vanadium Speciation

Vanadium on silica at submonolayer coverages has been studied by Scharaml-Marth *et al.* (19). Only at very low coverage (0.05%V, w/w) is vanadium present as monomeric tetrahedrally coordinated species VO_4^{3-}, linked to the support by three V–O–Si bridges and showing absorption bands at 254 (main band) and 294 nm. At 0.1%V on silica, vanadium is present as monomeric and oligomeric species and the absorptions are slightly red shifted. With increasing vanadium concentration one-dimensional chain-like surface species are developed which maintain tetrahedral coordination. At 0.5%V four bands are seen at 255, 279, and 289 nm and the main peak at 328 nm. At 1%V small clusters are formed, vanadium coordination increases, and the spectrum is red shifted. When the loading reaches 3.7%, small crystallites of V_2O_5 are detected and the main peak is located at 350 nm. It is clear that on silica as vanadium polymerizes, coordination increases, new bands appear, and the spectrum is red shifted.

The spectrum of all samples studied here, impregnated or exchanged, calcined to 300°C, presents a continuous absorption in the visible region assigned to polymeric chain structures related to V_2O_5. At 300°C the color of all samples is similar to that of vanadium pentoxide. At 500°C all samples are white or pale yellow. From the spectra and the color of the samples it is clear that at 500°C vanadium pentoxide structure-related compounds have disappeared. The temperature breaks chains and vanadium is spread out on the surface of the supports.

At 0.2%V on silica calcined at 700°C, vanadium must be present (19) as tetrahedral monomeric and oligomeric species. In Fig. 10, bands at 219 and 246 nm are assigned to monomeric species and the presence of some oligomers is detected by the shoulder around 300 nm.

The spectrum of 0.2%V on alumina calcined to 700°C is characterized by a broad peak at 287 nm (Fig. 11). The position and shape of this peak suggest that species present on alumina have higher molecular weight with wider distribution than the species present on silica. This assumption is consistent with the pale beige color of 0.2%V on alumina calcined at 700°C. It has been found that vanadium accumulates on alumina as small aggregates in FCC catalyst (16, 17).

Vanadium organic complexes of large organic ligands are too large to enter the zeolite pore structure when they are deposited by impregnation or in the FCC riser. At 300°C organic ligands of VBzA disappear and according to the spectra V^{V} is probably present in polymeric chains on the zeolite external surface. Temperature breaks chains and V^{V} migrates inside the zeolite, where it reaches acid sites as shown by ESR. The DRS spectra of impregnated and calcined at 700°C zeolites show similar bands as 0.2%V on silica (Fig. 10); however, the shape of the spectrum is different (see Figs. 6–9). The absorption around 300 nm indicates that some oligomeric tetrahedral species are still present. The main band of the spectra is the band at 212 nm, while the main band for vanadium on silica is located at 246 nm. The highest energy band is blue shifted in the spectra of vanadium on zeolites compared to vanadium on silica. This indicates that the coordination of monomeric species in zeolites is different from that of species found on silica. Vanadium in zeolites is present as cationic species as shown by ESR, while vanadium on silica has been found as anionic species like VO_4^{3-} (19). The predominant species of vanadium on zeolites calcined to 700°C is more likely VO_2^{+} than VO^{3+}, as the former can lose oxygen on heating in vacuum by the following reaction:

$$4\,VO_2^{+}Y \rightleftharpoons V_2O_4 + 2\,VO^{2+}Y + O_2. \qquad [3]$$

V_2O_4 could be responsible for the gray-black color observed after evacuation at 450°C of the samples calcined at 700°C.

From the spectra of fresh exchanged zeolites in Figs. 8 and 9, it is deduced that d–d transitions in V^{IV} are too weak to be identified in the calcined samples. The exchanged and calcined zeolites behave analogously to the impregnated samples; however, it is worth noting that even if the vanadium is located by ion exchange inside the zeolite, calcination at

300°C in an oxidizing atmosphere makes vanadium aggregate and polymerize. The reaction can be written as

$$2\,VO^{2+}\text{–Y} + H_2O + O_2 \rightarrow V_2O_5 + 2\,H^{+}\text{–Y}. \qquad [4]$$

The V_2O_5 produced is probably expelled to the zeolite external surface and is responsible for the brown color of the exchanged samples calcined to 300°C.

A comparison of spectra of the exchanged Z6 and Z7 zeolites calcined at 700°C (d spectra in Figs. 8 and 9) indicates that at this vanadium level there are differences in the coordination of the monomeric species present on the zeolites. The peak around 260 nm is more pronounced in Z6 exc. 0.82%V than in Z7 exc. 0.70%V; this is probably due to the presence of V^V anionic species on EFAL, confirming that EFAL can complex vanadium competing with the zeolite. The competition of EFAL and zeolite for vanadium explains the differences in the DRS spectra of Z6 and Z7 imp. 0.4%V samples calcined at 700°C and further evacuated at 450°C (Fig. 13). The spectra are characterized by strong bands in the visible region due to d–d transitions in the V_2O_4 formed. From Fig. 13 it is clear that the amount of vanadium reduced in Z6 was inferior to Z7 zeolite with the same vanadium content, treated in the same way. V^V deposited on EFAL in Z6 does not experience reduction under working conditions.

CONCLUSIONS

Our ESR and DRS results allow us to conclude that when vanadium is deposited on the external surface of zeolite Y it migrates and neutralizes acid sites. This migration is assisted by water, which is helpful but not indispensable. Vanadium mobility can be related to the low melting point of V_2O_5 (690°C). In the regenerator of a FCC plant the transportation of vanadium must be the result of the contribution of two mechanisms: the displacement by surface and gas phase transportation as vanadic acid formed according to Eq. [1] (10). However, in agreement with the calculus presented in the Introduction, the most important mechanism must be the migration on the surface.

At V levels normally found in FCC equilibrium catalyst, exchange is probably the first step in framework destruction. Acid site neutralization by vanadium in FCC catalysts has been previously observed (33).

These results agree very well with the activity measurements made by Torrealba and Goldwasser (17). They found that the high activity decay observed on 1%V impregnated zeolites cannot be explained completely by crystallinity reduction. This point is very important because it has been claimed that the vanadium problem in FCC can be solved by hardware modification of the unit (34). The idea has been to keep vanadium reduced during hydrogen combustion to avoid water and V^V contact, preserving zeolite crystallinity. We have shown here that before zeolite destruction there is ion exchange that probably reduces activity of the catalyst without damage to crystallinity.

The results of the exchanged and impregnated zeolites steamed in a reductive atmosphere allow us to conclude that V^{IV} does not play an important role in framework hydrolysis and that an oxidizing atmosphere is required for the catalytic action of vanadium. The damage of FCC catalysts must occur during the regeneration of the catalyst and not during the stripping, contrary to the proposal of Occelli (3). These results agree with those of Hettinger *et al.* (33), who concluded that the equilibrium catalyst is best simulated when air is introduced with the steam during catalyst deactivation in laboratory tests.

EFAL protects zeolite complexing vanadium as anionic species, harmless to the structure, delaying vanadium migration to the acid sites.

Mechanism

The mechanism for zeolite destruction by steam in the presence of vanadium under FCC process conditions can be summarized as follows:

V^V as a part of organic molecules is deposited on the catalyst external surface in the riser, where it is probably incorporated in the coke and transferred to the regenerator. Once in the regenerator the coke is burned off and vanadium is oxidized to V_2O_5. Vanadium pentoxide is a liquid under regenerator conditions. At low concentrations it can be easily spread out on the high-surface-area solid losing its solvent properties. Water helps vanadium mobilization by breaking V–O–Al and V–O–Si bonds and forming hydroxylated species. V^V has amphotheric behavior, so it can be presented as a neutral or positively charged species avoiding electrostatic repulsion from the negatively charged framework. In this way vanadium reaches acid sites, where it is trapped as cationic VO_2^+ species poisoning the catalyst according to the following reaction:

$$V_2O_5 + 2\,H^{+}\text{–Y} \rightleftharpoons 2\,VO_2^{+}\text{–Y} + H_2O. \qquad [5]$$

This is a dynamic equilibrium and its extent depends on temperature, water concentration, and acid site strength. The high temperatures found in the FCC regenerator favor the right side, but during hydrogen combustion water formed moves the equilibrium to the left and the vanadium pentoxide is able to produce vanadic acid according to Eq. [1]. The net reaction can be written as

$$VO_2^{+}\text{–Y} + 2\,H_2O \rightleftharpoons H^{+}\text{–Y} + H_3VO_4. \qquad [6]$$

Vanadic acid is a strong acid, $pK = 0.05$ (35). It is well known that acids catalyze framework hydrolysis, increasing the rate of dealumination. In this way the local vanadic acid concentration could be several orders of magnitude higher than predicted by Wormsbecher. This would explain zeolite framework hydrolysis by the weaker acid in lower bulk

concentration than sulfuric acid. This mechanism explains how small amounts of vanadium can cause large activity decays. In accordance with Pine (8), vanadium acts as a catalyst for zeolite framework hydrolysis because it is not consumed during zeolite destruction.

This mechanism explains almost all experimental results published in the field. V^V has a high tendency for polymerization; at higher concentrations than those currently found in FCC catalysts, liquid V_2O_5 formed can act as a solvent for zeolite components. In the presence of rare earths, vanadates can be formed after zeolite destruction. This mechanism, however, does not explain why two different species like sodium and vanadium produce similar effects on the zeolite and why both catalysts show synergistic action (8). To explain this fact, it is necessary to go further and propose a mechanism for zeolite dealumination. Kerr proposed the following scheme for zeolite dealumination (36–38):

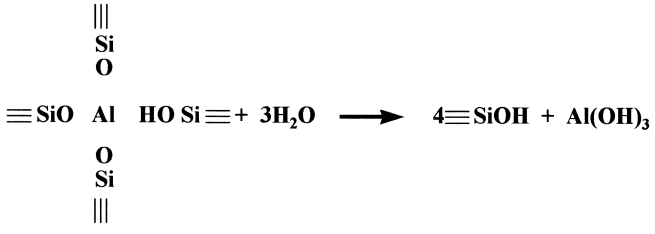

A more detailed mechanism can be the electrophillic attack of the hydronium ion on the negatively charged oxygen in the acid site:

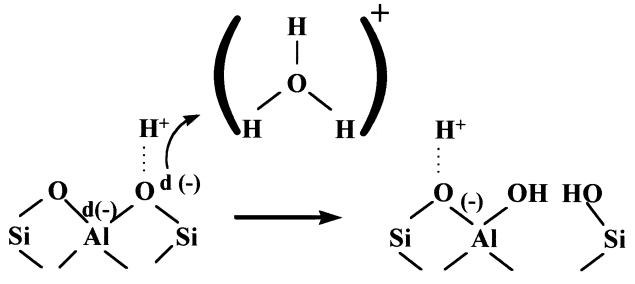

The net effect is the inclusion of a water molecule into the structure being catalyzed by the hydronium ion. From electronegativity considerations it is clear that if the charge compensating cation is a sodium the negative charge density on the oxygen will be higher than if it is a H^+. In the presence of sodium as a charge compensating cation the rate of hydrolysis would be higher and sodium and vanadium would present a synergistic effect in framework hydrolysis. Exchange of sodium by hydronium is not discharged; however, under FCC regenerator conditions there is not a solvent that facilitates it.

ACKNOWLEDGMENTS

C. A. Trujillo thanks Professor Pierre Jacobs for the opportunity to stay at the COK of the K. U. Leuven as a free researcher and for his invaluable help and orientation and also the Universidad Nacional de Colombia for the studies commission. P.P.K.G. thanks the National Fund for Scientific Research (NFWO) for a grant as research assistant. This research has been partially supported by Colciencias (Institution that promote the scientific and technological development in Colombia) and the Instituto Colombiano del Petróleo (ICP); their financial support is gratefully appreciated.

REFERENCES

1. Jaras, S., *Appl. Catal.* **2**, 207 (1982).
2. Venuto, P. D., and Habid, E. T., *Catal. Rev. Sci. Eng.* **18**, (1978).
3. Occelli, M. L., *Catal. Rev. Sci. Eng.* **33**, 241 (1991).
4. Agrawal, B. B., and Gulati, I. B., *Pet. Hydrocarbons* **6** (4), 193 (1972).
5. Wormsbecher, R. F., Peters, A. W., and Maselli, J. M., *J. Catal.* **100**, 130 (1986).
6. Occelli, M. L., "Akso Catalyst Symposium," p. 91. Scheveningen, The Netherlands, 1991.
7. Occelli, M. L., *in* "Fluid Catalytic Cracking: Role in Modern Refining. Vol. 375. ACS Symp. Series" (M. L. Occelli, Ed.), p. 343. ACS, Washington DC, 1989.
8. Pine, L. A., *J. Catal.* **125**, 514 (1990).
9. Nielsen, R. H., and Doolin, P. K., *J. Stud. Surf. Sci. Catal.* **76**, 339 (1993).
10. Sanchez, J. L., and Hager, J. P., *in* "EDP Congress 1993, Proceedings from the Symposium, TMS Annual Meeting" (J. P. Hager, Ed.), p. 655. Minerals Metals and Materials Society, Warrendale, PA, 1993.
11. Typical values for an UOP FCC unit in an Ecopetrol refinery at Barrancabermeja, Colombia.
12. Scherzer, J., "Octane-Enhancing Zeolitic FCC Catalysts. Scientific and Technical Aspects," p. 171. Dekker, New York, 1990.
13. Gallezot, P., Feron, B., Bourgogne, M., and Engelhard, Ph., *in* "Zeolites: Facts, Figures, Future" (P. A. Jacobs and R. A. Van Santen, Eds.), p. 1281. Elsevier, Amsterdam, 1989.
14. Mauge, F., Courcella, J. C., Engelhard, Ph., Gallezot, P., and Grosmangin, J., *J. Stud. Surf. Sci. Catal.* **28**, 803 (1986).
15. Mauge, F., Courcella, J. C., Engelhard, Ph., Gallezot, P., and Grosmangin, J., *in* "Proceedings, 7th International Zeolite Conference" (Y. Murakami, A. Iijima, and J. W. Ward, Eds.), p. 803. Kodanska, Tokyo, 1986.
16. Kugler, E. L., and Leta, D. P., *J. Catal.* **109**, 387 (1988).
17. Torrealba, M., and Golwasser, M. R., *Appl. Catal.* **90**, 35 (1992).
18. Anderson, M. W., Occelli, M. L., and Suib, S. L., *J. Catal.* **122**, 374 (1990).
19. Sharaml-Marth, M., Wokaun, A., Pohl, M., and Krauss, H.-L., *J. Chem. Soc. Faraday Trans.* **87**(16), 2635 (1991).
20. Huang, M., Shang, S., Yuan, C. L., and Wang, Q., *Zeolites* **10**, 772 (1990).
21. Lipness, B. C., and de Boer, J. H., *J. Catal.* **4**, 319 (1965).
22. Ballhausen, C. J., and Gray, B. H., *Inorg. Chem.* **1**, 111 (1962).
23. Hush, N. S., and Hobbs, J. M., *Prog. Inorg. Chem.* **10**, 277 (1968).
24. Blasco, T., Concepción, P., and López Nieto, J. M., Perez-Pariente, *J. Catal.* **152**, 1 (1995).
25. Lischke, G., Hanke, W., Jerschkewitz, H.-G., and Öhlmann, G., *J. Catal.* **91**, 54 (1985).
26. Centi, G., Perathoner, S., Trifiró, F., Aboukais, A., Aïssi, C. F., and Guelton, M., *J. Phys. Chem.* **96**, 2617 (1992).
27. Kucherov, A. V., and Slinkin, A. A., *Zeolites* **7**, 583 (1987).
28. Kucherov, A. V., and Slinkin, A. A., *Zeolites* **7**, 38 (1987).
29. Kucherov, A. V., and Slinkin, A. A., *Zeolites* **8**, 110 (1988).
30. Kucherov, A. V., and Slinkin, A. A., Beyer, G. K., and Borbely, G., *J. Chem. Soc. Faraday Trans.* **85**, 2737 (1989).
31. Garten, R. L., Delgass, W. N., and Boudart, M., *J. Catal.* **18**, 90 (1970).
32. McNicol, B. D., and Pott, G. T., *J. Catal.* **25**, 223 (1972).

33. Hettinger, W. P., Jr., Beck, H. W., Cornelius, E. B., Doolin, P. K., Kmecak, R. A., and Kovach, S. M., *Am. Chem. Soc. Div. Pet. Chem.* **28**(4), 920 (1983).
34. Myers, G. D., Hettinger, W. P., Jr., Kovach, S. M., and Zandona, O. J., US patent 4,432,863 (1984). Tatterson, D. F., and Ford, W. D., US patent 4,298,459 (1981).
35. Pope, M. T., *in* "Comprehensive Coordination Chemistry" (G. Wilkinson, Ed.), Vol. 3, p. 1026. Pergamon, Oxford, 1987.
36. Kerr, G. T., *J. Phys. Chem.* **72**, 2594 (1968).
37. Kerr, G. T., *J. Catal.* **15**, 200 (1969).
38. Kerr, G. T., *Adv. Chem. Ser.* **121**, 219 (1973).
39. Mitchell, B. R., *Ind. Eng. Chem. Prod. Res. Dev.* **19**, 209 (1980).
40. Clark, R. J., "The Chemistry of Vanadium and Titanium." Elsevier, 1968.
41. Hong, P.-K., Belford, R. L., and Pfluger, C. E., *J. Chem. Phys.* **43**(4), 1323, (9) 3111 (1965).